

Supplementary materials for

Hany A. ATALLAH, Rasha Hussein AHMED, Adel B. ABDEL-RAHMAN, 2024. Novel design of a compact tunable dual band wireless power transfer (TDB-WPT) system for multiple WPT applications. *Front Inform Technol Electron Eng*, 25(4):616-628. <https://doi.org/10.1631/FITEE.2200664>

1 DB J-inverter ECM

The corresponding circuit model of the proposed design and its result are extracted as shown in Fig. S1. The ground plane consists of two HR-DGSs to generate dual band operation at 1.6 GHz and tuned band as demonstrated in Fig. S1b. Therefore, $L_{P1} = L_{P2}$ and $C_{P1} = C_{P2}$ are related to the frequency of 1.6 GHz (ω_{01}). Likewise, $L_{P3} = L_{P4}$ and $C_{P3} = C_{P4}$ are related to the frequency of tuned band (ω_{02}). At this part, the equivalent circuit is analysed by employing the J-inverters method. Formerly, this method is employed to investigate a one band WPT design (Sharaf et al., 2019). However, at this work, it employed to investigate a DB-WPT system. Fig. S2a demonstrates the corresponding model of the proposed structure that functions at ω_{01} and ω_{02} that can be estimated by Eqs. (S1) and (S2) (Sharaf et al., 2019). Fig. S2b illustrates the essential components (J_{S1} , J_m , and J_{S2}) of the J-inverter method. Where J_{S1} , J_m , and J_{S2} represent the input, middle, and output J-inverters, consequently. The I/O J-inverters are associated with the coupling capacitors where the middle is associated with the mutual coupling. The incorporated essential components have the same magnitudes but with different signs to maintain the main circuit without any variation.

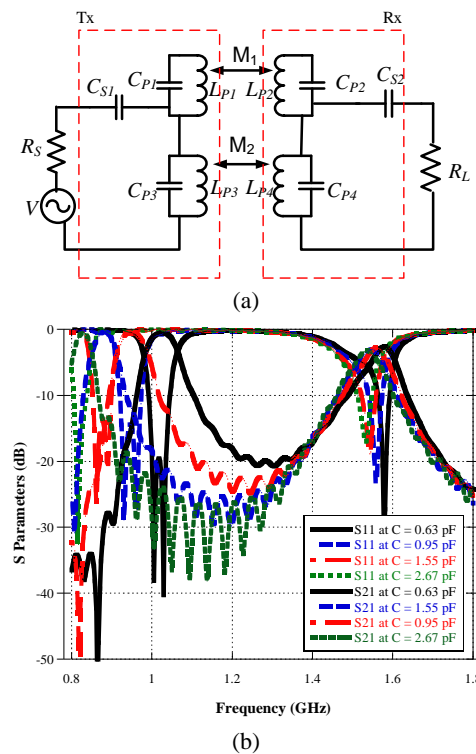


Fig. S1 Equivalent circuit of DB-WPT and results: (a) equivalent circuit of DB-WPT; (b) frequency response

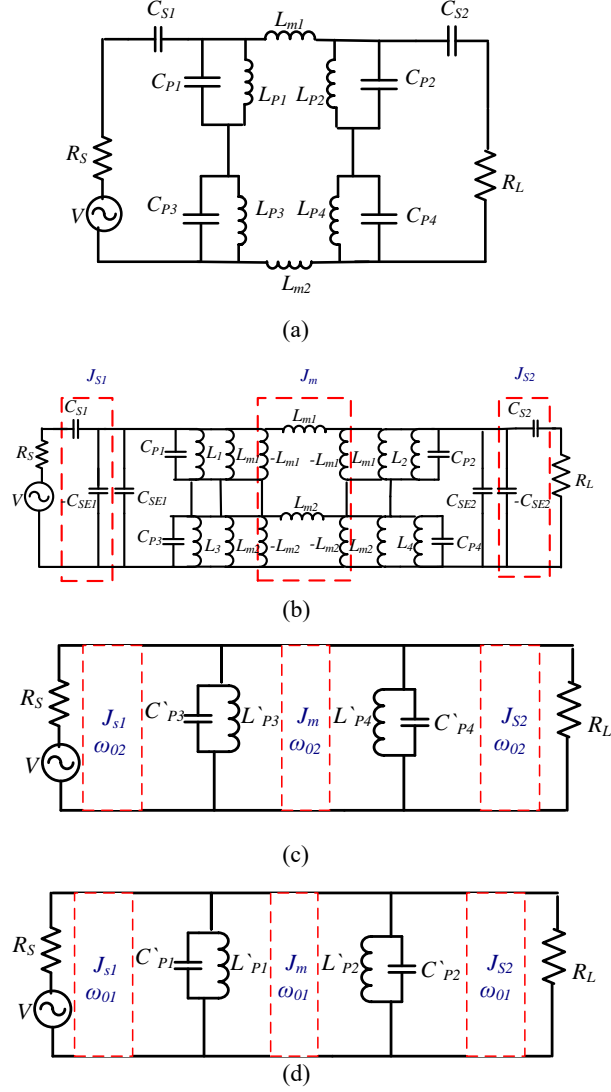


Fig. S2 Corresponding circuit using J-inverters: (a) π model; (b) using J-inverters; (c) at $\omega=\omega_{01}$; (d) at $\omega=\omega_{02}$

$$\begin{aligned}
 M_1 &= \frac{\text{Im}(Z_{12})}{2\pi f_{01}} = \frac{\text{Im}(Z_{21})}{2\pi f_{01}}, \\
 L_1 &= (L_{P1}L_{P2} - M_1^2) / (L_{P2} - M_1), \\
 L_2 &= (L_{P1}L_{P2} - M_1^2) / (L_{P1} - M_1), \\
 L_{m1} &= (L_{P1}L_{P2} - M_1^2) / M_1, \\
 C_{S1} &= \frac{J_{S1}}{\omega_{01}\sqrt{1-(J_{S1}R_0)^2}}, \\
 C_{S2} &= \frac{J_{S2}}{\omega_{01}\sqrt{1-(J_{S2}R_0)^2}}, \\
 C_{SE1} &= \frac{C_{S1}}{1+(\omega_{01}C_{S1}R_0)^2}, \\
 C_{SE2} &= \frac{C_{S2}}{1+(\omega_{01}C_{S2}R_0)^2}.
 \end{aligned} \tag{S1}$$

At $\omega = \omega_{02}$

$$\begin{aligned}
M_2 &= \frac{\text{Im}(Z_{12})}{2\pi f_{02}} = \frac{\text{Im}(Z_{21})}{2\pi f_{02}}, \\
L_3 &= (L_{P3}L_{P4} - M_2^2) / (L_{P4} - M_2), \\
L_4 &= (L_{P3}L_{P4} - M_2^2) / (L_{P3} - M_2), \\
L_{m2} &= (L_{P3}L_{P4} - M_2^2) / M_2, \\
C_{S1} &= \frac{J_{S1}}{\omega_{02}\sqrt{1-(J_{S1}R_0)^2}}, \\
C_{S2} &= \frac{J_{S2}}{\omega_{02}\sqrt{1-(J_{S2}R_0)^2}}, \\
C_{SE1} &= \frac{C_{S1}}{1+(\omega_{02}C_{S1}R_0)^2}, \\
C_{SE2} &= \frac{C_{S2}}{1+(\omega_{02}C_{S2}R_0)^2}.
\end{aligned} \tag{S2}$$

The chosen frequencies are isolated in the calculations because of the behaviour of the design. Fig. S2b is divided to two circuits as presented in Figs. S2c and S2d. Consequently, the elements of the circuits can be calculated using Eqs. (S3) and (S4).

$$\begin{aligned}
&\text{At } \omega = \omega_{01} \\
C_{P1} &= C_{P1} + C_{SE1}, \\
C_{P2} &= C_{P2} + C_{SE2}, \\
L_{P1} &= L_{P1} - \frac{M_1^2}{L_{P2}}, \\
L_{P2} &= L_{P2} - \frac{M_1^2}{L_{P1}}, \\
J_m &= 1 / (\omega_{01}L_{m1}).
\end{aligned} \tag{S3}$$

$$\begin{aligned}
&\text{At } \omega = \omega_{02} \\
C_{P3} &= C_{P3} + C_{SE1}, \\
C_{P4} &= C_{P4} + C_{SE2}, \\
L_{P3} &= L_{P3} - \frac{M_2^2}{L_{P4}}, \\
L_{P4} &= L_{P4} - \frac{M_2^2}{L_{P3}}, \\
J_m &= 1 / (\omega_{02}L_{m2}).
\end{aligned} \tag{S4}$$

2 Angular misalignment

Fig. S3 is discussed the angular misalignment between the Tx and the Rx at (90°, 180°, 270°, and 360°). In the worst case, more than half of the power is transferred from the Tx to the Rx at 90° and that is explained the benefit to use the symmetric shape of the system.

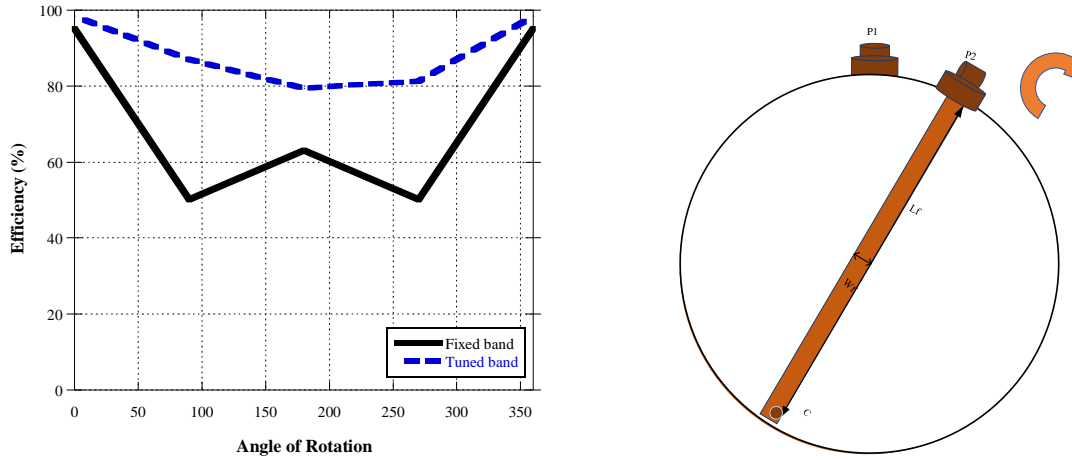


Fig. S3 Angular misalignment between Tx and Rx

3 Multiple WPT applications

The performance of the system is studied and investigated using multifunction transmitter where two receivers are employed as shown in Fig. S4a. The obtained simulation results are shown in Fig. S4. It is observed that the performance of the system is accepted for multi receivers and for multi applications.

Case 1

The result in Fig.S4b discusses the system where $C = 0.63$ pF in both Tx and Rx's, the performance of the system is accepted for multi receivers at the same resonance frequency.

Case 2

The results in Figs. S4c and S4d discuss the system with Tx is tuned ($C=0.63$ pF then $C=2.67$ pF), Rx_1 at $C=0.63$ pF and Rx_2 at $C=2.67$ pF, the performance of the system is accepted for multi receivers at different resonance frequencies.

Case 3

The results in Fig. S4e discuss the system with Tx with ($C=2.67$ pF), Rx_1 and Rx_2 at $C = 0.63$ pF, the receivers are coupled at only the fixed band at 1.6 GHz. Fig S4e is discussed the case when the Tx is adjusted at resonance frequency value away from the adjusted value of resonance frequencies of both the Rx_1 and Rx_2 . The two receivers cannot receive any signal from the Tx due to the difference in resonance frequencies. S_{21} parameter has to be a small value. S_{11} is presented the matched of the circuit in the Tx and the Rx.

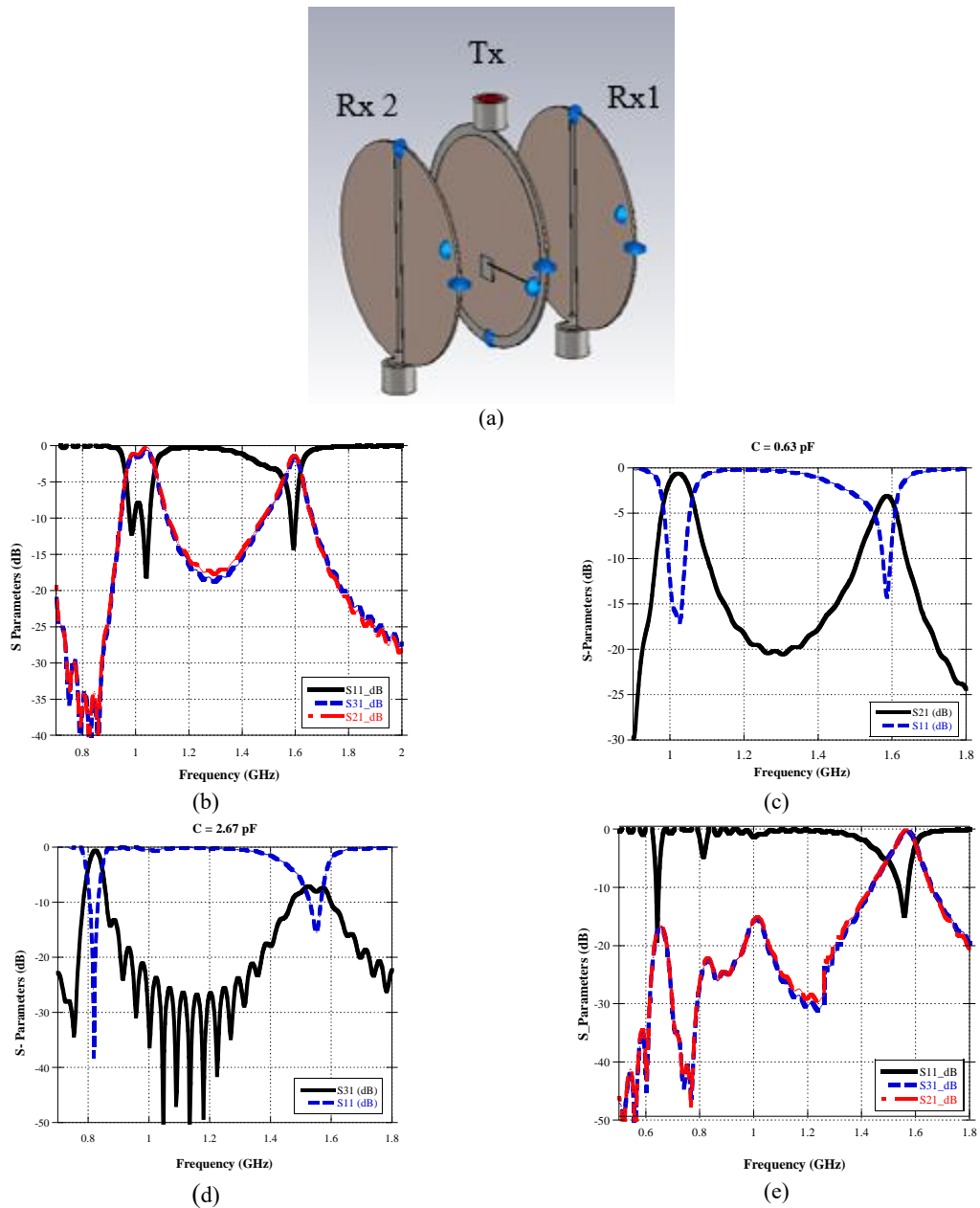


Fig. S4 Multiple WPT receivers: (a) Tx with Rx₁ and Rx₂; (b) frequency response for Case 1; (c) frequency response for Case 1; (d) frequency response for Case 2; (e) frequency response for Case 3

References

- Sharaf R, Abdel-Rahman AB, Abd El-Hameed AS, et al., 2019. A new compact dual-band wireless power transfer system using interlaced resonators. *IEEE Microw Wirel Compon Lett*, 29(7):498-500. <https://doi.org/10.1109/LMWC.2019.2917747>